

# Study of color centers in radiation-modified diamonds

M V Kozlova<sup>1,\*</sup>, A A Khomich<sup>2,\*\*</sup>, R A Khmelnskiy<sup>2,4</sup>, A A Averin<sup>5</sup>, A I Kovalev<sup>6</sup>,  
O N Poklonskaya<sup>6</sup>, I I Vlasov<sup>3</sup>, A V Khomich<sup>2</sup>, and V G Ralchenko<sup>3,7</sup>

<sup>1</sup> Physics Department, Moscow State University, Leninskie Gory, Moscow, 119991, Russia

<sup>2</sup> V. A. Kotelnikov Institute of Radio-Engineering and Electronics, Russian Academy of Sciences, pl. B. A. Vvedenskii, 1, Fryazino, Moscow Region, 141190, Russia

<sup>3</sup> A. M. Prokhorov Institute of General Physics, Russian Academy of Sciences, 38 Vavilova St., Moscow 119991, Russia

<sup>4</sup> P. N. Lebedev Institute of Physics, Russian Academy of Sciences, Leninsky prospect, 53, 119991, Moscow; Russia

<sup>5</sup> A. N. Frumkin Institute of Physical Chemistry and Electrochemistry, Russian Academy of Sciences, Leninsky prospect, 31/4, 119071, Moscow; Russia

<sup>6</sup> Physics Department, Belarusian State University, 4 Nezavisimosti Ave., Minsk, 220030, Belarus

<sup>7</sup> Harbin Institute of Technology, 92 Xidazhi Str., 150001 Harbin, P.R. China

\*E-mail: marija-kozlova@yandex.ru; \*\*e-mail: antares-610@yandex.ru

**Abstract.** We report on the optical properties of He-related color centers created by He-ion implantation and subsequent thermal annealing in natural diamonds, including the temperature (300–700 K) and excitation power (1–1800 kW/cm<sup>2</sup>)-dependent photoluminescence (PL) measurements. The prospects for the use of He-implanted diamonds for temperature sensing are discussed. The effect of fast neutron irradiation on the optical properties of Si-V color centers in CVD diamonds were also examined.

## 1. Introduction

Diamond, due to the availability of several classes of optically active defects (usually referred to as “color centers”), has been widely investigated as an attractive material for quantum optics and communication, quantum information processing, sensory and metrology applications [1]. The color centers in diamond are one of the most promising platforms for creating single-photon sources and spin qubits due to their outstanding photoluminescence properties: high quantum yields at room temperature, negligible photobleaching, short radiative lifetimes, narrow lines and absence of blinking [2]. The absence of cytotoxicity makes diamond with color centers attractive also as biomarkers. Ion implantation, electron or neutron irradiation with subsequent high-temperature annealing represent a powerful and flexible tool to engineer a broad range of different types of color centers in diamonds. The aim of this work is to study the properties of helium- and silicon-containing color centers in radiation-modified diamond.

## 2. Samples and experimental

Transparent polycrystalline (PCD) CVD diamond films of thickness > 500 μm and mean dimensions of crystallites ~ 50–70 μm have been grown on Si substrates from CH<sub>4</sub>/H<sub>2</sub> mixtures using a microwave plasma-enhanced CVD system ASTeX-PDS19 as described elsewhere [3]. The nitrogen concentration in the substitution position (determined as described in Ref. [3]) in the samples under the study was



$\sim 10^{18} \text{ cm}^{-3}$  and bound hydrogen content of  $2 \cdot 10^{19} \text{ cm}^{-3}$ . Free-standing PCD wafers were obtained by etching-off the Si substrate. After laser cutting and polishing to optical quality the samples were irradiated [4] in a wet channel of an IVV-2M nuclear reactor at  $325 \pm 10 \text{ K}$  by fast neutron flux of  $\sim 10^{14} \text{ cm}^{-2} \cdot \text{s}^{-1}$  (for energies  $> 0.1 \text{ MeV}$ ) at fluences  $F = 1 \times 10^{18}, 3 \times 10^{18}, 1 \times 10^{19}, 2 \times 10^{19}$  and  $2 \times 10^{20} \text{ cm}^{-2}$ . Polished plates of natural diamond were exposed to implantation with  $\text{He}^+$  ions with a set of energies (10 values ranging from the highest energy 350 keV to the lowest one 24 keV) and fluences that ensured uniform ( $\pm 10\%$ ) radiation damage in a 670-nm-thick layer. The implantation of helium ions was carried out on an ion accelerator “High Voltage Engineering Europa B.V.” (Netherlands). The samples were annealed in an oven with graphite walls, at a set of temperatures from 200 to 1700 °C for 60 min at each temperature in a vacuum of  $10^{-5} \text{ Torr}$ . Photoluminescence (PL) spectra were measured on LABRAM HR800 (Horiba) Raman spectrometer with laser excitation wavelengths of  $\lambda_{\text{ex}} = 473$  and 488 nm. The Linkam TS1500 minioven was used to study PL spectra at elevated temperatures.

### 3. Results and discussion

#### 3.1. Optical properties of He-implanted diamonds

Helium as a light ion is widely used to create diamond microstructures by ion implantation. Helium is considered to be chemically inert unlike reactive hydrogen, which, upon implantation and annealing, leads to blistering and explosive graphitization phenomena [5]. The crystal field of a superdense diamond lattice is so strong that even inert noble gas atoms, being placed in certain lattice positions, lose their chemical inertness and, due to the size effect [6], may form covalently bound defects with surrounding atoms, creating optically active centers.

The formation of color centers in natural diamond upon  $\text{He}^+$  implantation and subsequent annealing was discovered for the first time in the cathodoluminescence (CL) spectra [6, 7], where three strong narrow emission zero phonon lines (ZPL) at 560.5, 536.5, and 522.5 nm and a phonon sideband in the 563–620 nm spectral range were observed. The line at 522.5 nm sharply anneals out at  $t_{\text{an}} = 850 \text{ °C}$  and the helium-related lines at 536.5 nm (HR1) and 560.5 nm (HR2) simultaneously anneal out at 1200 °C [6]. The HR1 and HR2 bands were also observed in the electroluminescence [8] and PL [9, 10] spectra of MeV  $\text{He}^+$  ions implanted and annealed at 1000 °C synthetic diamonds. The spectral features of the HR1 and HR2 centers were studied as a function of several physical parameters, namely, the measurement temperature (25–300 K), the excitation wavelength, and the intensity of external electric fields. The HR1 and HR2 ZPLs could be effectively excited under both visible and UV radiation, these centers exhibit intense luminescence at excitation energies higher than the diamond band gap [10]. However, the suboptimal conditions for the HR center formation in combination with interfering high background PL due to nitrogen-vacancy (NV) centers with ZPL at 575 nm did not allow one to perform in [8–10] detailed studies of He-induced centers in diamond.

To study the PL spectra of helium-implanted diamonds, ten implantation cycles were performed for natural diamond plates with a set of energies (from 24 to 350 keV) and doses (from  $1.9 \times 10^{15}$  to  $6 \times 10^{15} \text{ cm}^{-2}$ ) to form a uniform radiation damage in a 670 nm thick layer with a total  $\text{He}^+$  dose of  $5 \times 10^{16} \text{ cm}^{-2}$  [11]. The formation of a layer with a uniform distribution of helium and the level of radiation damage made it possible to get rid of the manifestations of interference and to increase the signal-to-noise ratio in the PL spectra.

The HR1 and HR2 ZPLs were absent in the PL spectra after the implantation, appearing only after annealing at 550 °C (Fig. 1). In addition to the HR1 and HR2 ZPLs with their phonon sidebands, the PL spectra contain the diamond peak in Raman scattering at 522 nm and low-intensity background from the H3 centers (two nitrogen atoms separated by a vacancy) [12], located in the bulk of the sample (Fig. 1a). Besides, after heating to temperatures up to 675–900 °C, several sharp extra low-intensity bands were observed in the PL spectra (Fig. 1a), which anneal out at higher temperatures. Some of these bands appeared in CL spectra in [6]. For example, the band at 546 nm in its spectral position coincides with the L2 center reported [13] for ion-implanted diamonds, and a narrow band at 578 nm was previously observed in the PL spectra for ion-implanted and annealed type I diamonds with N3 ( $\text{N}_3\text{V}$ -defect) and H3 ( $\text{N}_2\text{V}$ -defect) centers [12]. With an increase in the annealing temperature, intensities of HR1 and

HR2 ZPLs grows in relation to the intensity of diamond Raman peak, reaching a maximum after annealing at  $\sim 950^\circ\text{C}$  (Fig. 1). After annealing step at  $950^\circ\text{C}$  (Fig. 1a, spectrum 5), the PL spectra contained only HR1 and HR2 ZPLs and 3H ZPL ( $<100>$  split-interstitial [12]) with respective phonon sidebands. A further increase in the annealing temperature led to a decrease in the intensity of HR1 and HR2 ZPLs (Fig. 1b). The relative intensities of the bands changed in a rather similar way, but not completely synchronously. Up to an annealing temperature of  $\sim 900^\circ\text{C}$ , the integral intensity of the HR1 band grew at a faster rate than that of HR2; however, with a further increase in the annealing temperature, the rate of extinction of the HR1 band exceeds that of HR2 (Fig. 1b). The HR1 and HR2 ZPLs have quite similar, but non-elementary spectral shape and consist of at least three different components, which was also reported in [6] and [10].

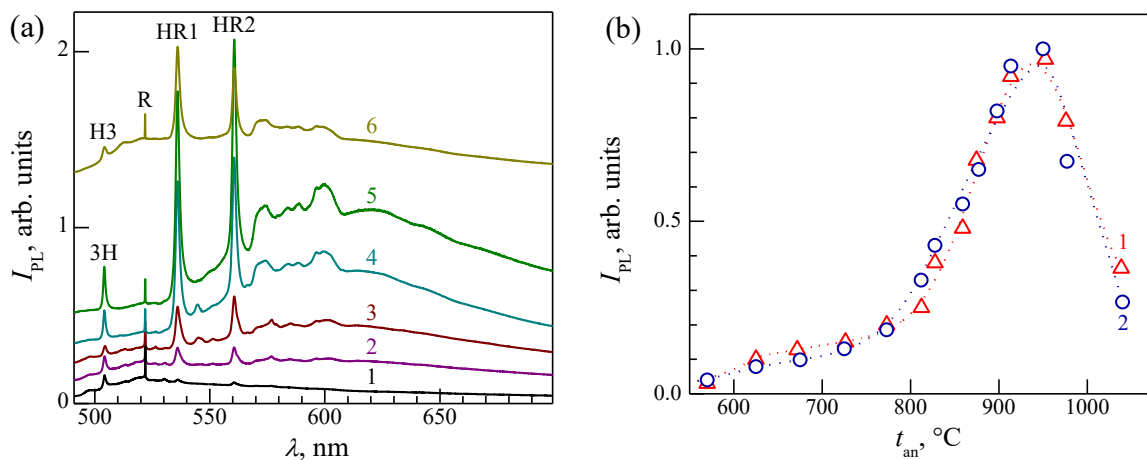


**Figure 1.** (a) Effect of annealing temperature on the PL spectra of natural diamond implanted with helium ions: 1 – 550, 2 – 625, 3 – 775, 4 – 877, 5 – 950, 6 – 1040  $^\circ\text{C}$ . For clarity, the spectra are shifted relative to each other vertically. All spectra are normalized by the integrated intensity of the Raman diamond band at 522 nm (denoted by R). The spectra were measured with excitation at  $\lambda_{\text{ex}} = 488 \text{ nm}$ ; (b) Integrated intensity of HR1 (triangles) and HR2 (circles) ZPLs as a function of the annealing temperature. The lines are the guides for an eye.

With an increase in the temperature of the measurements, the HR1 and HR2 ZPLs shifted to longer wavelengths and broadened, while the intensities of the ZPLs and their phonon sidebands decreased relative to the diamond Raman peak (Fig. 2). The HR1 band is more stable in the high measurement temperatures than HR2 and still can be observed in the PL spectrum measured at  $400^\circ\text{C}$ . The dependence of the full width at half maximum (FWHM) and the positions of the maxima (Fig. 2b) are typical for photoactive centers in diamond. The temperature softness for the HR1 and HR2 bands matches the temperature softness for the ideal crystal structure of diamond [12] to within 10%.

One of the promising applications is the use of color centers in diamonds for highly sensitive all-optical thermometry based on the temperature dependence of the fluorescence spectral shape [14]. The PL intensity, HWFM or position of the ZPL, Huang-Rhys factor can be exploited for sensing of temperature. Using multiparametric data analysis of the entire fluorescence spectral shape it is possible to receive a temperature sensitivity of  $13 \text{ mK}\cdot\text{Hz}^{-1/2}$  for SiV [15] and  $20 \text{ mK}\cdot\text{Hz}^{-1/2}$  for GeV [16]. The better developed SiV color center compared to the GeV has a narrower ZPL, but the GeV center has a nearly unitary quantum efficiency [17]. The use of helium-implanted diamonds with for thermometry also seems to be very promising. The HR1 and HR2 bands in terms of the Huang-Rhys factor, shift of the maxima and change of HWFM of ZPL with temperature are close to the same values for the SiV centers.

Ion implantation causes mechanical stresses in diamond [11]; however, we failed to notice a displacement of ZPL HR1 in the PL spectra (Fig. 2), whereas SiV ZPL can shift by several nanometers

due to mechanical stresses. Another advantage of HR1 centers is their high stability against laser excitation intensity. At the intensity  $W_{\text{ex}}$  as high as  $1 \text{ MW/cm}^2$ , no saturation of the HR1 band emission is observed (Fig. 3b), while for SiV centers the critical laser intensities are orders of magnitude lower [18]. The PL intensity of HR2 ZPL saturates at lower powers in comparison with that for HR1 (Fig. 3b), that could be one of the main reasons for variability of the HR1/HR2 intensity ratio, which was also observed in [6–10].

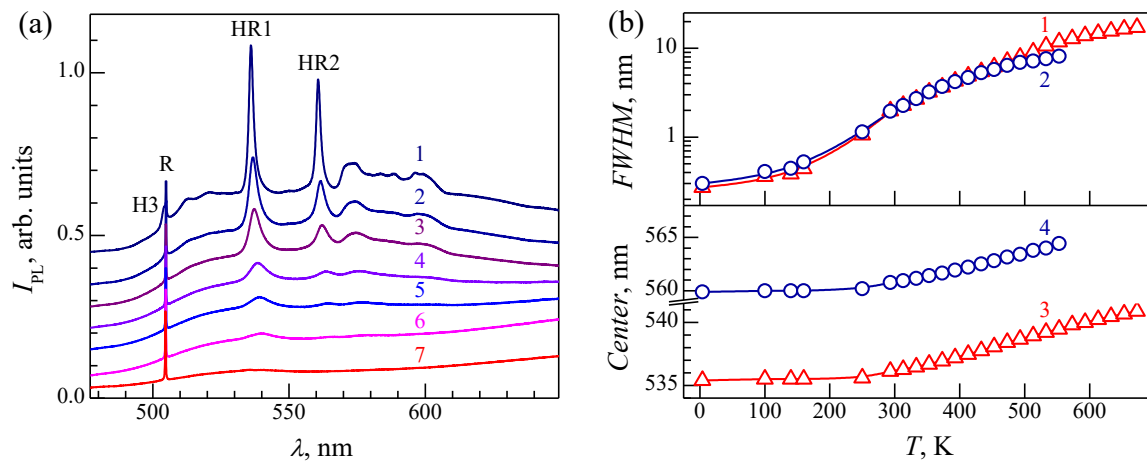


**Figure 2.** (a) The PL spectra of natural diamond implanted with helium ions (10 implantation cycles) with a total dose of  $5 \times 10^{16} \text{ cm}^{-2}$  and annealed at  $1040^\circ\text{C}$ , recorded at temperatures: 1 – 20, 2 – 100, 3 – 140, 4 – 220, 5 – 260, 6 – 300, 7 –  $400^\circ\text{C}$ . For clarity, the spectra are shifted relative to each other vertically. All spectra are normalized to integrated intensity of diamond band in the Raman spectra at 504 nm (denoted by R). The spectra were measured at  $\lambda_{\text{ex}} = 473 \text{ nm}$ . (b) Temperature broadening of ZPLs (top picture, curves 1 and 2) and shift (bottom picture, curves 3 and 4) of HR1 (triangles) and HR2 (circles) centers in PL for  $\text{He}^+$ -implanted natural diamond.

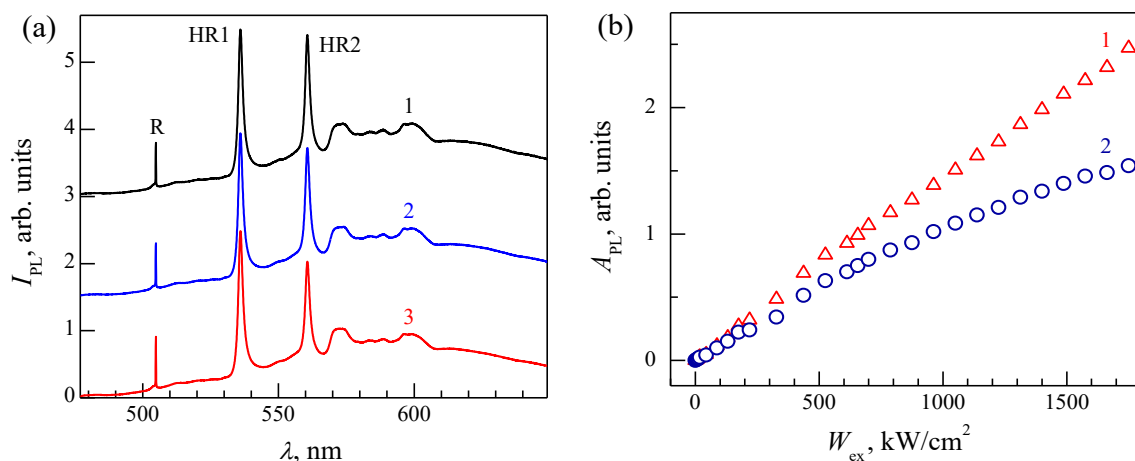


**Figure 3.** (a) PL spectra of helium-implanted and annealed at  $1040^\circ\text{C}$  natural diamond measured at different laser powers: 1 – 450, 2 – 1150 and 3 –  $1750 \text{ kW/cm}^2$ . The spectra are shifted relative to each other vertically. The spectra were measured at room temperature at  $\lambda_{\text{ex}} = 473 \text{ nm}$ ; (b) Dependence of integrated intensities  $A_{\text{PL}}$  of ZPL for HR1 (1 – triangles) and HR2 (2 – circles) centers on laser intensity  $W_{\text{ex}}$ .

More research is needed to establish the energy structure of He-induced HR1 and HR2 bands and to explore the benefits and limitations of their use as all-optical thermometric sensor.

### 3.2. SiV PL band in fast neutron irradiated CVD diamonds

The SiV defect, showing the strong luminescence with ZPL at 738 nm, is advantageous in terms of narrow ZPL ( $\approx 5$  nm), very weak vibronic sidebands, and short ( $\sim 1$  ns) lifetime at room temperature [19]. Ion implantation with subsequent annealing [20] or doping of CVD samples [21, 22] are used for the formation of the SiV centers. Here, we investigated the effect of neutron irradiation and subsequent annealing on the PL spectra of silicon-doped PCD CVD diamonds. In the samples irradiated with fast neutrons with fluences of  $1 \times 10^{18}$  and  $3 \times 10^{18}$   $\text{cm}^{-2}$ , SiV ZPL persists in the PL spectra after irradiation even before annealing (Fig. 4a); however, it significantly weakens and shifts to higher wavelengths (Fig. 4c). Its intensity is an order of magnitude higher than the GR1 (neutral single vacancy [12]) band, the presence of which in the PL spectra was taken into account when plotting the dependence in Fig. 4c. The subsequent annealing not only completely restores the position of the SiV band, but also significantly enhances its intensity. (Fig. 4a). Thus, after annealing at 1590 °C, the ratio of the amplitude of the SiV band to the amplitude of the diamond Raman peak reaches 250 (Fig. 4a), whereas in the pristine as-grown sample it was equal to 7. The NV centers in as-grown and in irradiated samples (ZPL at 575 nm [12]) upon annealing (Fig. 4a) transform into  $\text{N}_2\text{V}$  centers (H3 ZPL at 503.2 nm [12]).

With an increase in neutron fluence the degree of radiation damage to diamond is known to increase [23]. Particularly at higher dose of  $2 \times 10^{19}$   $\text{cm}^{-2}$  the SiV band appears in the PL spectrum only after annealing at 900–1000 °C (Fig. 4b) simultaneously with the ZPL of H19 center at 580 nm [24] (see inset in Fig. 4b). For this sample the position and shape of the SiV band is restored after annealing at 1650 °C, and its intensity increases significantly (Fig. 4b). Note, that for formation of SiV centers in diamond after ion implantation, lower annealing temperatures of 1000 °C [15] or 1100 °C [20] are usually chosen. For CVD diamonds under the study, the relationship between the shift and broadening of SiV ZPL is well described by a linear dependence, which makes it possible to judge on the degree of their radiation damage based on the shape of the PL spectrum of SiV centers in ion-implanted or neutron-irradiated diamonds.

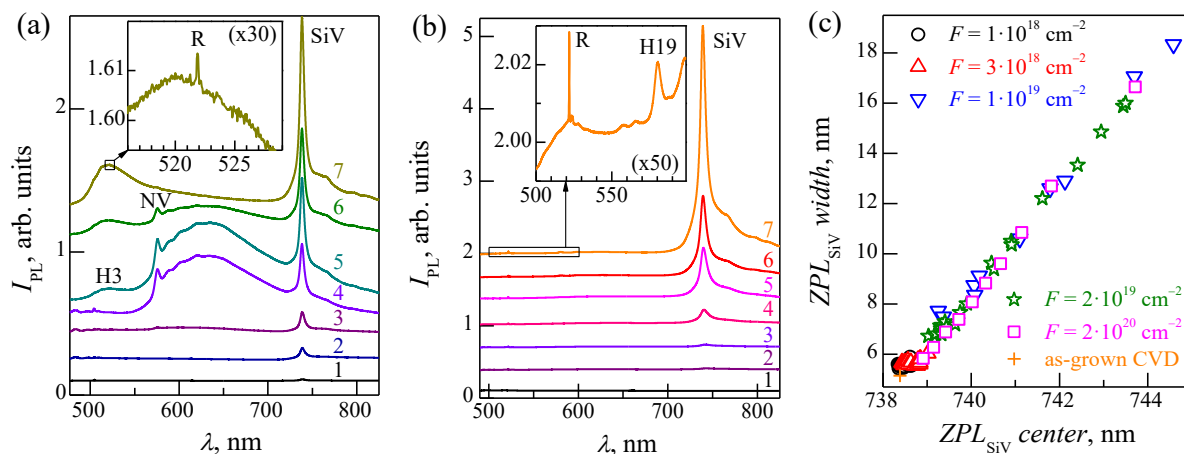


**Figure 4.** Transformations of the PL and Raman spectra of CVD diamonds irradiated with fast neutrons with fluences of  $1 \times 10^{18}$   $\text{cm}^{-2}$  (a) and  $2 \times 10^{19}$   $\text{cm}^{-2}$  (b) as a result of subsequent vacuum annealing at temperatures: 1 – 50, 2 – 550, 3 – 630, 4 – 800, 5 – 1370, 6 – 1480 and 7 – 1590 °C (a); and 1 – 50, 2 – 1080, 3 – 1150, 4 – 1375, 5 – 1520, 6 – 1620 and 7 – 1660 °C (b), respectively. All spectra are normalized to the integrated intensity of the diamond band in the Raman spectra (denoted by R). The spectra were measured at  $\lambda_{\text{ex}} = 488$  nm and shifted relative to each other vertically for clarity. (c) Correlation of measured spectral position and width of SiV ZPL as result of annealing of CVD diamonds, irradiated with neutrons at different fluences  $F = 1 \times 10^{18}$  (circles),  $3 \times 10^{18}$  (triangles up),  $1 \times 10^{19}$  (triangles down),  $2 \times 10^{19}$  (stars) and  $2 \times 10^{20}$  (squares)  $\text{cm}^{-2}$ . The cross shows the position and FWHM of SiV ZPL in pristine as-grown un-irradiated CVD diamond film.

#### 4. Conclusion

Multienenergetic implantation of helium ions and subsequent annealing make it possible to form He-containing color centers in diamonds, which appear in the PL spectra in the form of narrow bands in the 500–600 nm range. An optimal annealing temperature of 950 °C is found to lead in two brightest and most thermally stable bands at ~536 and ~560 nm (HR1 and HR2). The similarities and differences in the behavior of the ZPLs HR1 and HR2 are revealed in dependence of the annealing temperature, the intensity of the exciting radiation, and the temperature in the PL spectra measurements. It has been demonstrated that fast neutron irradiation and subsequent annealing at 1600 °C makes it possible to increase the PL of SiV centers in CVD diamonds by orders of magnitude. A correlation has been established between the spectral shift and broadening of the SiV ZPL in fast neutron irradiated diamonds, which makes it possible to use the parameters of SiV ZPL as a measure of the radiation damage degree in ion-implanted and in fast neutron irradiated diamonds.

#### Acknowledgments

The authors are grateful to K. Boldyrev for measuring the PL spectra at low temperatures. This work was supported by Russian Science Foundation, grant no. 20-72-00122 (SiV centers study), Russian Foundation for Basic Research, grant no. 20-52-04002 and Belarusian Republican Foundation for Fundamental Research, grant no. F21RM-137.

#### References

- [1] Bradac C, Gao W, Forneris J, Trusheim M E and Aharonovich I 2019 *Nat. Commun.* **10** 5625
- [2] Pezzagna S, Rogalla D, Wildanger D, Meijer J and Zaitsev A 2011 *New J. Phys.* **13** 035024
- [3] Nistor S V, Stefan M, Ralchenko V, Khomich A and Schoemaker D 2000 *J. Appl. Phys.* **87** 8741-8746
- [4] Karkin A E, Voronin V I, Berger I F, Kazantsev V A, Ponosov Yu S, Ralchenko V G, Konov V I and Goshchitskii B N 2008 *Phys. Rev. B* **78** 033204
- [5] Khmelniitskiy R A, Zavedeev E V, Khomich A V, Gooskov A V and Gippius A A 2005 *Vacuum* **78** 273-279
- [6] Tkachev V D, Zaitsev A M and Tkachev V V 1985 *Phys. Stat. Sol. (b)* **129** 129-133
- [7] Gippius A A, Vavilov V S, Zaitsev A M and Zhakupbekov B S 1983 *Physica B* **116** 187-194
- [8] Forneris J *et al.* 2015 *Nucl. Instrum. Meth. Phys. Res. B* **348** 187-190
- [9] Forneris J *et al.* 2016 *J. Luminesc.* **179** 59-63
- [10] Prestopino G *et al.* 2017 *Appl. Phys. Lett.* **111** 111105
- [11] Khmelniitskiy R A, Dravin V A, Tal A A, Latushko M I, Khomich A A, Khomich A V, Trushin A S, Alekseev A A and Terentiev S A 2013 *Nucl. Instrum. Meth. Phys. Res. B* **304** 5-10
- [12] Zaitsev A M 2001 *Optical Properties of Diamond: A Data Handbook*, Springer, Berlin
- [13] John R, Lehnert J, Mensing M, Spemann D, Pezzagna S and Meijer J 2017 *New J. Physics* **19** 053008
- [14] Fujiwara M and Shikano Y. 2021 *Nanotechnology* **32** 482002
- [15] Choi S, Agafonov V N, Davydov V A and Plakhotnik T 2019 *ACS Photon.* **6** 1387-1392
- [16] Blakely S M *et al.* *ACS Photonics* 2019 **6** 1690-1693
- [17] Fan J W *et al.* 2018 *ACS Photonics* **5** 765-770
- [18] Gao Y F *et al.* 2018 *J. Phys. Chem. Lett.* **9** 6656-6661
- [19] Vlasov I I, Barnard A S, Ralchenko V G, Lebedev O I, Kanzyuba M V, Saveliev A V, Konov V I and Goovaerts E 2009 *Adv. Mater.* **21** 808-812
- [20] Lagomarsino S *et al.* 2018 *Diam. Rel. Mater.* **84** 196-203
- [21] Bolshakov A P *et al.* 2015 *Phys. Stat. Sol. (a)* **212** 2525-2532
- [22] Sedov V, Ralchenko V, Khomich A A, Vlasov I, Vul A, Savin S, Goryachev A and Konov V 2015 *Diam. Rel. Mater.* **56** 23-28
- [23] Khomich A A, Khmelniitskiy R A and Khomich A V 2020 *Nanomaterials* **10** 1166
- [24] Khomich A A *et al.* 2019 *J. Appl. Spectr.* **86** 597-605